[CANCER RESEARCH 60, 3921–3926, July 15, 2000]

# Histone H3 and Heat Shock Protein GRP78 Are Selectively Cross-Linked to DNA by Photoactivated Gilvocarcin V in Human Fibroblasts[1]

**Akira Matsumoto[2] and Philip C. Hanawalt**

*Department of Radiation Biophysics and Genetics, School of Medicine, Kobe University, 650-0017 Kobe, Japan [A. M.], and Department of Biological Sciences, Stanford University, Stanford, California 94305-5020 [P. C. H.].*

## ABSTRACT

**Gilvocarcin V (GV) is an antitumor antibiotic with a coumarin-based aromatic structure that promotes protein-DNA cross-linking when photoactivated by near-UV light. We have now identified several proteins that are selectively cross-linked to DNA in human fibroblasts by photoactivated GV, using $NH_2$-terminal amino acid sequencing and Western blot analysis of the purified cross-linked proteins. The selectively cross-linked proteins are histone H3 and GRP78, a heat shock protein belonging to the heat shock protein-70 family. The hydrophobic leader sequence is missing from the cross-linked GRP78, suggesting that only the processed form of the protein is cross-linked to DNA. It is primarily the phosphorylated form of histone H3 that is cross-linked to DNA. Gel retardation analysis from four different GV-treated human fibroblast cell lines revealed two distinct shifted bands, and subsequent immunoblotting confirmed *in situ* that the slower and the faster bands, respectively, contained GRP78 and histone H3 cross-linked to DNA. The selective cross-linking of these particular proteins is dependent on UV irradiation in the presence of GV, which may help to clarify the unique molecular mechanism of this potent antitumor agent.**

## INTRODUCTION

The gilvocarcins were originally isolated from *Streptomyces gilvotanalens* fermentation medium (1, 2), and they harbor a common chromophore composed of four fused planar rings, including a coumarin backbone (Fig. 1). The antitumor and virus-killing efficiency of gilvocarcins depend on the alkyl group in the C-8 position (3–5). It has been shown that gilvocarcin with a vinyl-group in this position, GV,[3] has enhanced biological activity (5–7). Biological activities such as cell killing, prophage induction, mutagenesis, and DNA strand break formation in both bacteria (7, 8) and mammalian cells (9, 10) require photoactivation of the gilvocarcin by UVA, UVB, or visible light (6, 7, 9). Very low concentrations of photoactivated GV are biologically active, and the cellular target for GV includes DNA (11, 12). A covalent photoadduct of GV to DNA has been isolated *in vitro* and identified as a thymine-GV adduct (13, 14). We have previously used a modified Southern blot analysis to detect interstrand DNA cross-linking (15) in specific DNA sequences. We found that the GV lesions represented DNA-to-protein cross-linking rather than interstrand DNA cross-linking in several genes studied (16).

The objective of the present study was to identify the specific protein(s) cross-linked to DNA by photoactivated GV. Identification of these proteins may help to clarify the molecular mechanism of this potent antitumor antibiotic.

Received 3/8/99; accepted 5/11/00.

The costs of publication of this article were defrayed in part by the payment of page charges. This article must therefore be hereby marked *advertisement* in accordance with 18 U.S.C. Section 1734 solely to indicate this fact.

[1] Supported by a Grant-in-Aid for Scientific Research from the Ministry of Education, Science, Sports and Culture, Japan (to A. M.) and Grant CA44349 from the United States National Cancer Institute (to P. C. H).

[2] To whom requests for reprints should be addressed, at Department of Radiation Biophysics and Genetics, School of Medicine, Kobe University, 7-5-1 Kusunoki-cho, Chuo-ku, 650-0017 Kobe, Japan. Phone: 81-78382-5601; Fax: 81-66705-5806.

[3] The abbreviations used are: GV, gilvocarcin V; HSP, heat shock protein.

## MATERIALS AND METHODS

**Cell Culture and Photoactivated GV Treatment.** Four normal human diploid fibroblast cell lines were used: (*a*) GM637 and GM38 (Human Genetic Mutant Cell Depository, Camden, NJ); and (*b*) NHDF and NHLF (Takara, Osaka, Japan). Cells were grown at 37°C in modified Eagle's essential medium supplemented with 10% fetal bovine serum at 37°C in a humidified atmosphere containing 5% $CO_2$. The culture medium was changed twice weekly. Prepared GV was dissolved in DMSO and stored at −20°C. Monolayer cells growing in 82-mm culture dishes were washed twice with cold PBS (2.68 mM KCl, 1.47 mM $KH_2PO_4$, 8.06 mM $Na_2HPO_47H_2O$, and 0.137 M NaCl). The cells were then treated with 0.3 $\mu$g/ml GV in 2 ml of PBS. After a 5-min equilibration in the dark at 4°C, a portion of the cell culture was irradiated with fluorescent "black light" (HP15L; ATTO, Kusatsu, Japan) at 1.0 kJ/$m^2$/min for 15 min; control cells were covered with a light shield and were not irradiated. The cells were then washed three times with cold PBS and lysed for DNA preparation.

**Preparation and Separation of Proteins Cross-Linked to DNA and $NH_2$-terminal Amino Acid Sequencing.** Proteins cross-linked to DNA were prepared using potassium-SDS precipitation, which uses the difference between SDS and potassium in protein precipitation properties (17, 18). Cells were scraped with a rubber policeman, washed three times in ice-cold PBS, and then pelleted and resuspended in ice-cold PBS to a concentration of $5 \times 10^6$ cells/ml. After centrifugation at 3000 × *g* for 10 min, approximately $2 \times 10^8$ cells were lysed in 25 ml of 20 mM Tris-HCl (pH 7.5), 2% SDS, and 1 mM phenylmethanesulfonyl fluoride. The lysed sample was vortexed for 20 s and warmed to 65°C for 15 min, and 25 ml of 20 mM Tris-HCl (pH 7.5) and 200 mM KCl were added. The mixture was then passed rapidly through a 5-ml plastic pipette five times. The SDS-potassium precipitate was formed by cooling the sample on ice for 10 min and collected by centrifugation at 3000 × *g* for 10 min at 4°C. The pellet was dispersed and suspended in 5 ml of 20 mM Tris-HCl (pH 7.5) and 100 mM KCl by pipetting five times. The sample was heated for 15 min at 65°C, chilled on ice, and centrifuged at 3000 × *g* for 10 min, followed by repetition of the washing step three times. The resulting pellet, which is enriched with proteins associated with DNA, was resuspended in 5 ml of sterile water and then used for the following two analyses. Because the pellet contained nonspecific proteins precipitated by SDS, it was dissolved in 20 mM Tris-HCl (pH 7.5)/50 mM NaCl and then immunoprecipitated with an antihuman double-strand DNA antibody using protein A-Sepharose beads. The immunoprecipitate was suspended in 20 mM Tris-HCl (pH 7.5), kept at 65°C for 20 min, and passed through a protein A-Sepharose affinity column to remove the antibody. The obtained eluant was condensed using a lyophilizer and then mixed with an equal amount of the SDS sample buffer of Tris-glycine SDS-PAGE (19). Separation and precise calibration of low molecular weight proteins were conducted using the Tris-tricine gel system SDS-PAGE (20). Marker proteins for calibration were as follows: (*a*) phosphorylase b, 94 kDa; (*b*) albumin, 67 kDa; (*c*) ovalbumin, 43 kDa; (*d*) carbonic anhydrase B, 30 kDa; (*e*) trypsin inhibitor, 20.1 kDa; (*f*) $\alpha$-lactoalbumin, 14.4 kDa; (*g*) myoglobin I and III, 10.7 kDa; and (*h*) myoglobin I, 0.82 kDa (Amersham Pharmacia, Buckinghamshire, United Kingdom). Separated proteins were detected by Coomassie Brilliant Blue R-250 (Bio-Rad) staining.

In the scaled-up experiment for amino acid sequencing, it was sometimes difficult to resuspend the pellet due to an excess amount of SDS and potassium salts. To remove these, the suspension was dialyzed overnight against 1 liter of sterile distilled water. This reduced the amount of residual undissolved material and also removed nonspecific SDS-protein precipitate. The final precipitate was dissolved in 10 mM Tris-Cl (pH 7.5) and 1 mM EDTA and applied to a limit filtration column (Amersham Pharmacia) to trap proteins with molecular masses larger than 100 kDa. The same volume of SDS sample buffer used in the Laemmli gel system was added to the final pass-through fraction of the

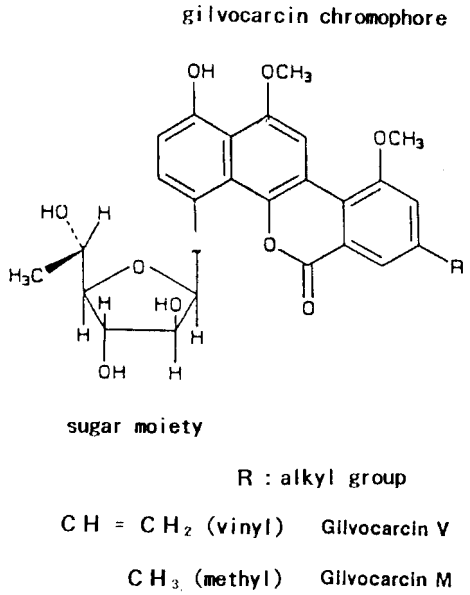


Fig. 1. Structure of gilvocarcins.

above-mentioned column, boiled for 5 min, and applied to a 10% SDS-PAGE gel. After electrophoresis at 15 mA constant current for 4 h, the gel was soaked in a 3-(cyclohexylamino)propanesulfonic acid blotting buffer [10 mM 3-(cyclohexylamino)propanesulfonic acid and 10% methanol] for 15 min. The gel was then electroblotted onto a polyvinylidene difluoride membrane (Immobilone P$^{SQ}$; Millipore) using a semidry blotting apparatus (21). The blot filter was then stained with Coomassie Brilliant Blue R-250. After washing by vigorous vortexing in 50% methanol, the stained band was subjected to Edman degradation using a Procise$^{TM}$ Model 492 peptide sequencer (Applied Biosystems).

**Preparation of High Molecular Weight DNA without Proteinase K Treatment and Gel Retardation Analysis Using Modified Immunoblotting.** Approximately $2 \times 10^6$ washed cells were lysed at 37°C for 16 h with 5 ml of lysis buffer consisting of 10 mM Tris-Cl (pH 8.0), 1 mM EDTA, and 0.5% SDS. To avoid loss of DNA-linked protein, DNA samples were prepared without proteinase K treatment; instead, sodium deoxycholate was added to 0.2 M (final concentration) of the lysate. The lysate was then extracted with phenol, phenol/chloroform, chloroform/isoamyl-alcohol, and ether. Precipitated DNA was then dissolved in TE buffer [10 mM Tris-Cl (pH 8.0) and 1 mM EDTA] and treated with 100 $\mu$g/ml pancreatic RNase A. To avoid artifactual effects due to visible light exposure, these procedures were conducted under yellow light, and all samples were shielded by aluminum foil. A portion of high molecular weight DNA prepared from each of four human fibroblast cell lines was exhaustively digested with *Eco*RI (Takara) and then loaded in the parallel well of neutral agarose gel (15). The separation profile was detected and photographed using a camera-ready UV transilluminator (Kodak). Transfer to a sheet of Hybond C nitrocellulose membrane (Amersham), which has binding capacities for both DNA and proteins, was then performed using a modified method in which 0.05 M NaOH was used for denaturation, an electroblotter (ATTO) was used for transfer instead of osmotic blotting, and blotting was completed within 1 h. After washing the Hybond C filter with three changes of PBS for 15 min each, it was subjected to the immunoblot detection procedure described below.

**Antibodies.** Anti-GRP78 goat polyclonal antibody (Santa Cruz Biotechnology) was raised against a peptide corresponding to amino acids 24–43 mapping at the $NH_2$ terminus of the 78-kDa glucose-regulated protein (GRP78) precursor. An anti-phosphorylated histone H3 rabbit polyclonal antibody (Upstate Biotechnology) was raised against a peptide corresponding to amino acids 7–20 of human histone H3 with phosphorylated serine at residue 10.

## RESULTS

**Detection and Purification of Proteins Cross-Linked to DNA by Photoactivated GV in Human Diploid Fibroblasts.** Proteins cross-linked to DNA were prepared from control cells, cells treated with GV without UVB irradiation, or cells treated with photoactivated GV.

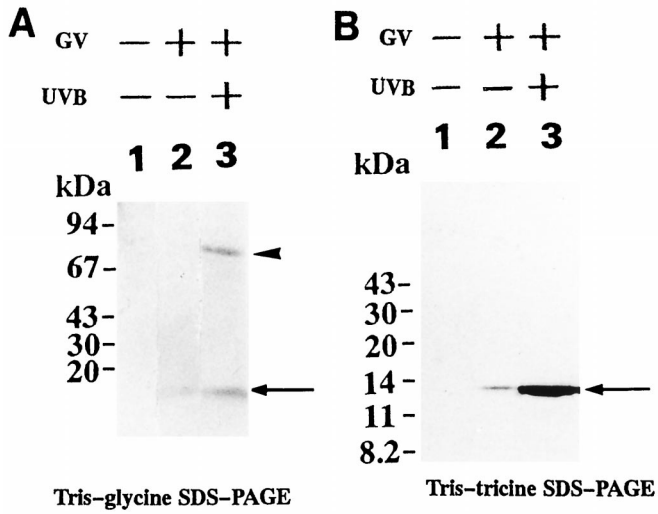


Fig. 2. Preparation of cross-linked proteins to DNA induced by photoactivated GV in human fibroblasts (GM637). *A*, separation of two cross-linked proteins using the SDS-PAGE Tris-glycine gel system. Sample prepared from control cells (*Lane 1*), sham-irradiated cells with GV (*Lane 2*), or UVB-irradiated cells with GV (*Lane 3*) was mixed with the same amount of the SDS sample buffer, boiled for 5 min, and loaded on wells for SDS-PAGE. After electrophoresis, the gel was stained with Coomassie Brilliant Blue R-250. *B*, precise separation of the low molecular mass cross-linked protein using the SDS-PAGE Tris-tricine gel system. Samples were the same as those described in *A*, except that each sample was passed through a limit filtration column (Ultrafree 30) to remove proteins with molecular mass higher than 30 kDa and that the passed-through sample was mixed with the same amount of the sample buffer of Tris-tricine SDS-PAGE at 37°C for 15 min instead of boiling. *Left*, migration positions of high molecular weight (*A*) or low molecular weight (*B*) calibration markers in each gel system. *Arrowhead*, migration position of the 78-kDa protein in Tris-glycine SDS-PAGE; *arrows*, the positions of the 13-kDa protein in both gel systems.

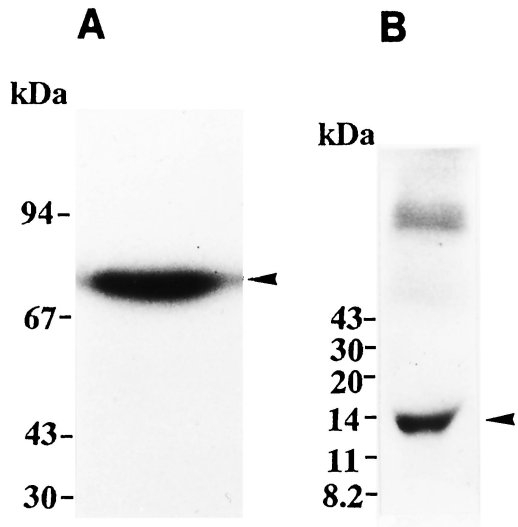


Fig. 3. Preparation of cross-linked proteins for $NH_2$-terminal amino acid sequencing. Approximately 60 pmol (total) of the prepared cross-linked protein were separated by either Tris-glycine SDS-PAGE to isolate the 78-kDa protein (*A*) or Tris-tricine SDS-PAGE to isolate the 13-kDa protein (*B*). Each gel was then transferred to an Immobilon$^{PSQ}$ membrane and stained with Coomassie Brilliant Blue. The protein band corresponding to each molecular mass was cut out and subjected to Edman degradation analysis. *Left*, migration positions of molecular mass markers. *Arrowheads*, migration position of the 78-kDa protein (*A*) and the 13-kDa protein (*B*), respectively.

Table 1 *Edman degradation profile of the 78-kDa protein cross-linked by photoactivated GV*

The yield of the respective amino acid residue in each cycle is presented in pmol. The amino acid that exhibited the largest recovery is underlined. Amino acid residues are abbreviated as follows: D, aspartic acid; E, glutamic acid; N, asparagine; S, serine; T, threonine; Q, glutamine; G, glycine; H, histidine; A, alanine; Y, tyrosine; R, arginine; P, proline; M, methionine; V, valine; W, tryptophane; K, lysine; F, phenylalanine; I, isoleucine; L, leucine.

| | Cycle no. | | | | | | | | | | | | | | | | |
|---|---|---|---|---|---|---|---|---|---|---|---|---|---|---|---|---|---|
| Amino acid | 1 | 2 | 3 | 4 | 5 | 6 | 7 | 8 | 9 | 10 | 11 | 12 | 13 | 14 | 15 | 16 | 17 |
| D | 2.6 | 3.4 | 36.1 | 2.7 | 2.9 | 3.8 | 33.2 | 3.1 | 2.4 | 2.0 | 2.6 | 2.9 | 3.6 | 3.1 | 22.4 | 2.4 | 2.0 |
| E | 33.4 | 30.6 | 4.9 | 3.6 | 3.0 | 32.7 | 3.9 | 3.0 | 2.4 | 2.0 | 2.5 | 3.6 | 3.0 | 2.1 | 2.4 | 3.4 | 2.7 |
| N | 2.1 | 2.6 | 2.0 | 0.9 | 1.8 | 1.6 | 2.8 | 2.4 | 1.4 | 1.2 | 1.8 | 2.4 | 1.3 | 2.5 | 2.1 | 1.4 | 1.6 |
| S | 1.1 | 1.6 | 2.2 | 0.6 | 1.3 | 2.1 | 1.6 | 1.8 | 2.4 | 2.3 | 1.3 | 1.8 | 2.0 | 3.1 | 2.1 | 1.6 | 1.8 |
| T | 0.8 | 1.1 | 1.6 | 0.4 | 1.7 | 1.4 | 0.7 | 1.6 | 1.3 | 19.3 | 2.5 | 2.0 | 1.5 | 1.8 | 2.0 | 1.2 | 1.8 |
| Q | 3.5 | 2.6 | 1.8 | 2.0 | 2.6 | 2.4 | 1.8 | 1.4 | 1.6 | 1.9 | 2.0 | 2.7 | 2.4 | 1.8 | 1.4 | 1.9 | 1.8 |
| G | 4.2 | 4.1 | 4.0 | 3.8 | 3.9 | 3.6 | 3.4 | 3.2 | 28.8 | 5.6 | 4.0 | 3.6 | 23.5 | 3.9 | 4.1 | 3.5 | 23.4 |
| H | 1.6 | 0.8 | 0.7 | 1.6 | 1.1 | 1.2 | 0.9 | 0.8 | 1.8 | 2.0 | 2.4 | 1.5 | 1.7 | 1.9 | 0.7 | 1.2 | 1.6 |
| A | 4.1 | 3.5 | 3.9 | 3.2 | 4.4 | 3.7 | 3.2 | 3.3 | 2.9 | 3.7 | 4.4 | 4.2 | 3.6 | 3.1 | 2.9 | 3.8 | 3.9 |
| Y | 1.5 | 1.3 | 1.0 | 0.8 | 1.1 | 1.5 | 1.6 | 2.0 | 1.6 | 1.9 | 2.9 | 2.5 | 2.0 | 1.5 | 2.7 | 1.8 | 1.6 |
| R | 3.2 | 2.8 | 2.9 | 3.0 | 1.9 | 2.7 | 2.9 | 3.0 | 3.4 | 3.7 | 2.7 | 2.2 | 3.6 | 3.2 | 1.9 | 2.5 | 3.7 |
| P | 2.9 | 3.0 | 2.2 | 2.1 | 2.6 | 2.3 | 3.0 | 3.4 | 3.6 | 2.9 | 2.2 | 2.6 | 2.5 | 2.1 | 1.9 | 2.6 | 2.9 |
| M | 2.5 | 2.1 | 1.8 | 2.0 | 1.3 | 0.6 | 0.9 | 1.4 | 2.1 | 2.4 | 2.6 | 1.6 | 1.8 | 2.1 | 2.5 | 2.2 | 1.5 |
| V | 3.8 | 3.1 | 2.1 | 2.7 | 3.1 | 2.0 | 3.6 | 25.8 | 5.0 | 4.1 | 22.4 | 20.9 | 4.9 | 4.1 | 3.4 | 3.1 | 2.7 |
| W | 0 | 0 | 0 | 0 | 0 | 0 | 0 | 0 | 0 | 0 | 0 | 0 | 0 | 0 | 0 | 0 | 0 |
| K | 2.4 | 2.1 | 0.9 | 19.8 | 17.8 | 3.9 | 3.1 | 2.0 | 1.9 | 2.1 | 2.3 | 2.6 | 1.4 | 1.4 | 2.8 | 2.3 | 2.1 |
| F | 1.9 | 1.2 | 0.7 | 0.4 | 1.3 | 1.2 | 1.0 | 1.5 | 2.4 | 2.1 | 1.5 | 1.5 | 1.2 | 2.3 | 1.2 | 1.6 | 1.8 |
| I | 3.5 | 3.1 | 2.1 | 2.8 | 2.5 | 2.1 | 1.9 | 2.1 | 2.9 | 3.1 | 2.7 | 2.4 | 1.4 | 23.8 | 4.6 | 3.1 | 2.8 |
| L | 2.5 | 2.1 | 1.5 | 1.7 | 1.8 | 1.1 | 0.8 | 0.4 | 1.3 | 2.5 | 2.6 | 2.3 | 2.2 | 2.6 | 1.7 | 21.6 | 3.4 |

SDS-PAGE separation profiles of the three samples were obtained from $1.5 \times 10^5$ cells of each sample as shown in Fig. 2. No cross-linked protein was detected in the control samples within the sensitivity limits of Coomassie Brilliant Blue staining (Fig. 2*A*, *Lane 1*). The sample obtained from cells treated with 0.3 $\mu$g/ml GV and in sham-irradiated conditions exhibited a trace amount of a 13-kDa band (Fig. 2*A*, *Lane 2*). The sample obtained from cells treated with 0.3 $\mu$g/ml photoactivated GV exhibited two distinct bands of 78 kDa and ~10 kDa in the Tris-glycine gel system SDS-PAGE (Fig. 2*A*, *Lane 3*). Each band appeared monodisperse. Because the migration position of the smaller band in Tris-glycine SDS-PAGE is beyond the range of proportional distribution in the molecular mass, the sample was passed through a filtration limit column to remove proteins with molecular masses exceeding 30 kDa and then separated by using Tris-tricine system SDS-PAGE to more accurately determine the molecular mass of the smaller protein band (Fig. 2*B*). The molecular mass of the smaller cross-linked protein is 13 kDa, judging from its migration position in relation to the protein markers (Fig. 2*B*, *Lane 3*).

**$NH_2$-terminal Amino Acid Sequencing of Two Cross-Linked Proteins.** To identify the two distinct proteins detected in the above-mentioned analysis, a larger-scale experiment was performed. GM637 cells ($5 \times 10^6$ ) treated with 0.3 $\mu$g/ml photoactivated GV were used as a starting material, and approximately 60 pmol (total) of the 78-kDa protein were isolated by Tris-glycine SDS-PAGE (Fig. 3*A*), and the same amount of the 13-kDa protein was isolated by Tris-tricine SDS-PAGE (Fig. 3*B*), blotted onto a polyvinylidene difluoride membrane, and visualized by Coomassie Brilliant Blue staining. The results of each sequential Edman degradation profile expressed as the recovery of each cycle in pmol for the 78-kDa protein band are presented in Table 1, and the results of each sequential Edman degradation profile expressed as the recovery of each cycle in pmol for the 13-kDa protein band are presented in Table 2.

**Deduced Amino Acid Sequence Alignment with a Sequence Identified in the Protein Database.** A homology search of two protein databases, PIR and SWISS-PROT, using each amino acid sequencing result in Table 1 showed that the $NH_2$-terminal 17-amino

Table 2 *Edman degradation profile of the 13-kDa protein cross-linked by photoactivated GV*

The yield of the respective amino acid residue in each cycle is presented in pmol. The amino acid that exhibited the largest recovery is underlined. Amino acid residues are abbreviated as follows: D, aspartic acid; E, glutamic acid; N, asparagine; S, serine; T, threonine; Q, glutamine; G, glycine; H, histidine; A, alanine; Y, tyrosine; R, arginine; P, proline; M, methionine; V, valine; W, tryptophane; K, lysine; F, phenylalanine; I, isoleucine; L, leucine.

| | Cycle no. | | | | | | | | | | | | | | | | |
|---|---|---|---|---|---|---|---|---|---|---|---|---|---|---|---|---|---|
| Amino acid | 1 | 2 | 3 | 4 | 5 | 6 | 7 | 8 | 9 | 10 | 11 | 12 | 13 | 14 | 15 | 16 | 17 |
| D | 1.6 | 1.4 | 1.2 | 0.6 | 1.6 | 2.1 | 1.9 | 2.4 | 2.3 | 1.7 | 3.8 | 2.3 | 2.1 | 2.5 | 2.1 | 2.1 | 1.9 |
| E | 2.5 | 2.3 | 2.6 | 3.2 | 2.6 | 3.6 | 3.8 | 3.1 | 2.1 | 1.8 | 1.5 | 2.4 | 2.4 | 2.7 | 2.1 | 2.6 | 2.2 |
| N | 0.8 | 0.6 | 2.1 | 1.5 | 1.5 | 1.7 | 0.6 | 0.9 | 1.4 | 1.6 | 2.1 | 1.6 | 0.6 | 1.4 | 1.5 | 1.2 | 1.4 |
| S | 1.4 | 1.6 | 1.7 | 1.3 | 1.3 | 2.6 | 1.4 | 1.9 | 2.4 | 21.8 | 3.9 | 2.5 | 2.5 | 2.2 | 1.8 | 2.1 | 1.8 |
| T | 1.0 | 1.6 | 17.4 | 2.8 | 2.0 | 19.2 | 3.0 | 2.3 | 1.4 | 2.1 | 19.9 | 3.4 | 2.7 | 2.1 | 1.8 | 1.9 | 2.5 |
| Q | 3.1 | 2.7 | 2.3 | 1.9 | 22.4 | 3.6 | 3.1 | 2.6 | 2.8 | 1.9 | 2.7 | 2.2 | 2.4 | 2.6 | 1.8 | 2.1 | 1.5 |
| G | 3.4 | 3.1 | 3.6 | 2.4 | 2.7 | 1.9 | 2.6 | 1.4 | 1.8 | 2.1 | 2.8 | 27.4 | 23.7 | 4.1 | 3.6 | 3.7 | 3.6 |
| H | 2.1 | 1.4 | 1.5 | 1.8 | 0.9 | 2.1 | 1.6 | 1.7 | 1.1 | 1.4 | 1.8 | 0.6 | 0.7 | 1.2 | 1.4 | 1.6 | 1.6 |
| A | 24.6 | 5.6 | 3.9 | 3.6 | 3.1 | 3.8 | 23.1 | 4.5 | 3.2 | 2.8 | 3.9 | 2.5 | 3.7 | 3.8 | 21.4 | 3.9 | 2.1 |
| Y | 1.2 | 0.9 | 0.5 | 0.7 | 1.1 | 1.0 | 1.4 | 1.6 | 0.8 | 1.2 | 1.5 | 1.2 | 1.1 | 1.5 | 0.6 | 1.4 | 0.7 |
| R | 2.6 | 15.8 | 4.6 | 3.1 | 3.4 | 3.1 | 3.5 | 17.9 | 4.8 | 3.7 | 3.6 | 3.1 | 3.2 | 2.9 | 2.7 | 2.9 | 14.3 |
| P | 2.1 | 2.3 | 1.9 | 2.5 | 2.3 | 2.1 | 3.1 | 3.6 | 2.6 | 2.8 | 1.5 | 2.3 | 2.8 | 3.1 | 3.6 | 25.3 | 4.1 |
| M | 5.1 | 4.5 | 3.5 | 3.2 | 3.4 | 3.1 | 3.6 | 2.8 | 2.5 | 3.1 | 3.7 | 3.2 | 3.1 | 2.4 | 2.9 | 3.1 | 2.4 |
| V | 3.2 | 2.6 | 2.7 | 2.9 | 2.4 | 2.1 | 3.1 | 3.2 | 2.7 | 3.2 | 3.6 | 2.5 | 2.9 | 3.2 | 3.5 | 3.8 | 3.5 |
| W | 0 | 0 | 0 | 0 | 0 | 0 | 0 | 0 | 0 | 0 | 0 | 0 | 0 | 0 | 0 | 0 | 0 |
| K | 3.5 | 3.6 | 3.5 | 25.7 | 4.1 | 3.8 | 4.2 | 3.6 | 23.8 | 4.7 | 3.8 | 3.6 | 3.5 | 20.9 | 4.6 | 4.3 | 3.8 |
| F | 3.2 | 2.5 | 2.7 | 3.1 | 1.9 | 2.5 | 2.1 | 1.6 | 1.7 | 2.3 | 2.0 | 1.8 | 3.1 | 2.7 | 1.7 | 1.6 | 1.7 |
| I | 2.4 | 2.1 | 1.8 | 1.9 | 2.1 | 3.1 | 2.7 | 2.4 | 1.7 | 2.5 | 2.8 | 2.5 | 2.1 | 1.9 | 1.6 | 2.1 | 2.7 |
| L | 2.3 | 2.1 | 1.8 | 1.5 | 2.4 | 2.7 | 1.9 | 1.8 | 2.4 | 1.6 | 2.7 | 1.5 | 1.9 | 2.2 | 2.4 | 1.8 | 1.4 |

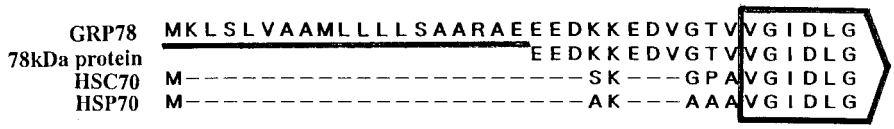


Fig. 4. Alignment of the $NH_2$-terminal amino acid sequence of the 78-kDa protein with those of GRP78 and other stress-70 family HSPs of human origin. Sequences are aligned to obtain maximum homology. The hydrophobic leader sequence of GRP78 is *underlined*. The $NH_2$-terminal portion of the putative ATP binding domain common to these proteins is *boxed*.

acid sequence of the 78-kDa protein was identical to that of the GRP78 protein, without the hydrophobic leader sequence (Fig. 4), and that the $NH_2$-terminal 17-amino acid sequence of the 13-kDa protein completely matched that of the mammalian histone H3.

**Western Blot Analysis of Two Proteins Cross-Linked by Photoactivated GV.** To further identify the prepared cross-linked proteins, these proteins were separated by either Tris-glycine or Tris-tricine SDS-PAGE, and each gel was blotted onto a polyvinylidene difluoride membrane sheet. Cross-linked protein on the membrane was then detected immunologically by Western blot analysis using anti-GRP78 antibody (Fig. 5*A*) or anti-phosphorylated histone H3 antibody (Fig. 5*B*). The major 78-kDa band was detected in all preparations of cross-linked human fibroblast proteins derived from three different sources (GM637, NHDF, and NHLF) on treatment with photoactivated GV (Fig. 5*A*, *Lanes 2–4*). In cells treated with sham-irradiated GV, however, only a trace amount of the protein band was detected (Fig. 5*A*, *Lane 5*). In all three samples treated with photoactivated GV, a trace amount of the 70-kDa band was detected (Fig. 5*A*, *Lanes 2–4*). Although the nature of this protein band is unknown at present, this protein seems to cross-react with the epitope in 24–43 amino acid residues at the $NH_2$-terminal portion of GRP78, against which the polyclonal antibody was raised. No cross-reactive band signal was detected using anti-phosphorylated histone H3 antibody. Although the 13-kDa band is detected most sensitively and specifically by this antibody, another antibody that recognizes overall histone H3 detects the band quite insensitively (data not shown). Note that other band signals corresponding to histone H2A, H2B, and H4 were not detected.

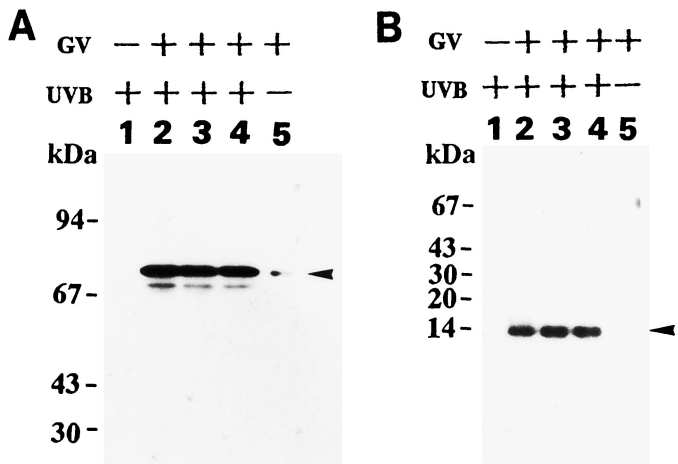


Fig. 5. Western blot analysis of proteins prepared by the method to enrich DNA-cross-linked proteins from various human fibroblasts treated with photoactivated GV. Protein samples were prepared from GM637 (*Lanes 1, 4,* and *5*), GM38 (*Lane 2*), and NHDF-Ad (*Lane 3*). Conditions for cell exposure to GV were control experiment without GV (*Lane 1*), experiments with photoactivated GV (*Lanes 2–4*), or experiment with sham-irradiated GV (*Lane 5*). Polyclonal antibodies used were antihuman GRP78 antibody (*A*) and antihuman phosphorylated histone H3 antibody (*B*). *Left*, migration positions of molecular mass markers. *Arrowheads*, migration positions of GRP78 (*A*) and phosphorylated histone H3 (*B*), respectively.

**Gel Retardation Analysis of GV-treated Fibroblasts from Various Sources and Immunoblot Detection *in Situ*.** To obtain direct evidence that the two identified proteins prepared by the SDS-potassium precipitation method are actually unique as DNA-cross-linked proteins in GV-treated human fibroblasts, we used native agarose gel separation of endonuclease-cleaved high-molecular weight DNA prepared without proteinase K treatment. Using *Eco*RI to cleave the DNA, separation of DNA fragments by neutral agarose gel electrophoresis effectively revealed two distinctive retarded bands in all four human fibroblast DNA samples tested (Fig. 6*A*). To minimize the denaturing effect for the epitopes expressed in the cross-linked proteins, a modified blotting procedure to a nitrocellulose filter membrane was used as described above. This enabled identification *in situ* of the cross-linked proteins in all four human fibroblasts as GRP78 (Fig. 6*B*) and histone H3 (Fig. 6*C*). Neither retarded bands nor these immunoreactive protein bands were detected in control samples prepared with proteinase K (Fig. 6, *Lanes 1*) or in those treated in the absence of GV (Fig. 6, *Lanes 2*) or UVB (Fig. 6, *Lanes 3*).

## DISCUSSION

Two independent methods were used for identification of the selectively cross-linked proteins: (*a*) preparation of enriched DNA-cross-linked proteins followed by both amino acid sequencing and immunological detection; and (*b*) *in situ* identification of the DNA-cross-linked proteins by immunological detection. The first method left some uncertainty regarding the relationship of the two prepared proteins to the two retarded bands originally found in the GV-treated fibroblasts (16). The second method has inherent weakness regarding the stability of epitope(s) of protein that is detected immunologically. Fortunately, identification of the faster-moving band as histone H3, a protein rich in basic amino acids, was successful, possibly due to its stability in alkali (Fig. 6*C*). However, immunological detection of the slower-moving band as GRP78 appears as a weak single band signal (Fig. 6*B*). This suggests that some epitopes expressed on GRP78 are alkali-labile, and only the stable epitopes are detected by the anti-GRP78 polyclonal antibody. Taken together, the results indicate that the primary target proteins in human fibroblasts for DNA-to-protein cross-linking induced by photoactivated GV are GRP78 and histone H3. Failure to detect these retarded bands in samples prepared with proteinase K and in those treated under incomplete conditions for the cross-link formation also supports the significance of the gel retardation analysis.

**GRP78, A Stress-70 (HSP-70) Family Protein Lacking the Hydrophobic Leader Sequence, Is a Target Protein for DNA-to-Protein Cross-Linking Induced by Photoactivated GV.** HSPs are synthesized when cells are exposed to hyperthermia or to certain toxic chemicals (22). The most abundant and well conserved of these is the stress-70 (HSP-70) protein family. GRP78, a member of this family that is abundantly expressed in the lumen of the endoplasmic reticulum, was originally found independently as an immunoglobulin heavy chain-binding protein in myeloma cells (23) and as a glucose regulated protein whose synthesis rate is increased by glucose starvation or

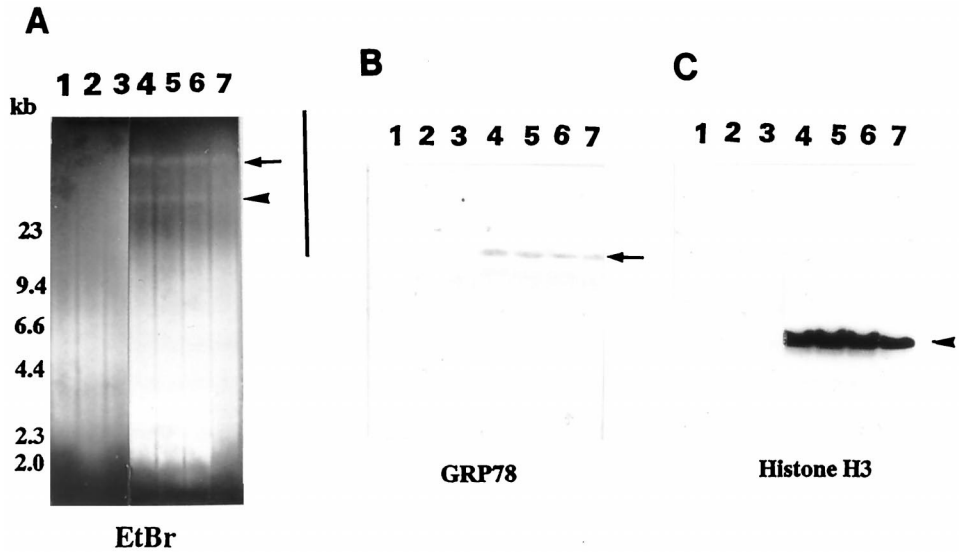


Fig. 6. Gel retardation analysis of the cross-linked DNA prepared from various human fibroblasts. Cross-linked DNA samples were prepared with (*Lanes 1*) or without proteinase K treatment (*Lanes 2–7*), and some samples were prepared in the absence of GV (*Lanes 2*) or UVB (*Lanes 3*). *Lanes 1, 2, 3* and *7*, NHLF; *lanes 4*, GM637; *lanes 5*, GM38; *lanes 6*, NHDF-Ad. *Arrows* and *arrowheads* on the *right* indicate migration positions of the slower-moving and the faster-moving bands, respectively. *A*, separation profile of each *Eco*RI-digested DNA by neutral agarose gel electrophoresis visualized by ethidium bromide (*EtBr*) staining under a UV transilluminator. *Left*, migration positions of DNA molecular mass markers in kb. The *vertical bar* on the *right* indicates the region of the neutral gel run in parallel with *A* and immunoblotted. *B* and *C*, immunoblot detection of the unstained agarose gel using anti-GRP78 antibody (*B*) or anti-phosphorylated histone H3 antibody (*C*).

a variety of stress conditions (24). Like other HSP-70 proteins, the likely function of GRP78 binding protein is to recognize unfolded polypeptides and proteins and, by inhibiting intra- or intermolecular aggregation, maintain them in a state competent for subsequent refolding and oligomerization (25). The GRP78 protein is also directly or indirectly involved in the translocation of secretory precursors across the endoplasmic reticulum membrane (26).

The SDS-PAGE profile of the 78-kDa protein appears as a single homogeneous protein band (Fig. 2), and the $NH_2$-terminal amino acid sequencing result also indicates that the cross-linked protein is GRP78 protein without the hydrophobic leader sequence, which is always found in the lumen of endoplasmic reticulum. HSP-70 family proteins are, in general, expressed in the mammalian cell nucleus and cytosol. The leader sequence has been clearly shown to be a tissue-specific determinant of subcellular distribution (27). Munro *et al.* (28) transfected COS cells with GRP78 cDNA, with or without the 5′ sequence that encodes the hydrophobic leader sequence, and then analyzed the subcellular GRP78 distribution in cells. Cells transfected with the cDNA containing the hydrophobic leader sequence exhibited a typical granular expression pattern in cytosol, suggesting specific expression in the endoplasmic reticulum. However, cells transfected with GRP78 cDNA lacking the hydrophobic leader sequence exhibited a typical nuclear distribution similar to that of endogeneous HSP-70 expression and that of *Drosophila* HSP-70 when expressed in the same cells (29). Note that in this study, GRP78 with the leader sequence was not detected as a GV-cross-linked protein, as verified by $NH_2$-terminal amino acid sequencing (Table 1). However, the reason for the selective cross-linking of GRP78 with DNA by this DNA-damaging agent remains unknown. Because it has been shown that the moiety reactive to DNA in photoactivated GV is the C-8 position of the vinyl group (30), the other reactive moiety that bridges the GRP78 protein and photoactivated GV may be certain amino acid residues with photoactivatable aromatic side chains, such as tryptophan. Photoactivation by UVB irradiation may then induce both reactive moieties of GV and particular amino acids of proteins, and the specific proteins that are closely associated with DNA will be cross-linked.

**Histone H3 as Protein DNA Cross-Linked by Photoactivated GV.** The nucleosome consists of DNA wound around a histone octamer containing two molecules each of core histones H2A, H2B, H3, and H4. The histone octamer plays a passive role in efficient DNA packaging, an important role in DNA replication and transcription (31, 32). Secondary modification of histones, such as acetylation and phosphorylation, is closely associated with these roles (33). Specific cross-linking of histone H3, but not of other histones, is associated with the molecular characteristics of photoactivated GV. Thus, the interaction is not simply a nonspecific one occurring in amine-rich proteins such as histones. One explanation could be that the distance and three-dimensional position between DNA and the reactive group of histone H3 matches well with the molecular structure of photoactivated GV. Of the four core histones, H3 and H4 can form nucleosome-like structures by themselves, and both are evolutionarily conserved. The $NH_2$ terminus of histone H3 extends 10–20 amino acids further from the nucleosome core (34). In the histone-DNA cross-linking analysis, histone H3 and histone H4 show different cross-linking patterns along the nucleosomal DNA, in which histone H3 but not histone H4 (35) associates with DNA that is both entering and exiting the nucleosome, suggesting that histone H3 associates with the entry and exit DNA or linker DNA in its vicinity. Interestingly, phosphorylation of the $NH_2$-terminal domain of histone H3 is correlated with activation of *jun* and *fos* (36). Because the antibody used in our analysis detects the phosphorylated form of histone H3 (Figs. 5*B* and 6*C*), this finding suggests a possible relevance of the antitumor activity of photoactivated GV.

Formaldehyde preferentially cross-links histones to DNA (37) because amine-rich proteins are the favored substrates for formaldehyde cross-linking to amine positions of unpaired DNA bases. (37, 38). Although the group of the photoactivated GV that is reactive to the target protein has not yet been identified, it must differ from the activated vinyl group at the C-8 position that reacts with DNA (30). The cross-linking formation mechanism thus appears to differ from that of the formaldehyde-histone cross-linking, which involves the same reactive group present in both DNA and protein.

**DNA-to-Protein Cross-Linking, DNA Damage with Potent Biological Activity, and Significance of Target Protein Identification.** Formaldehyde, *cis*-platinum, and trivalent chromate are known to be carcinogenic in animals, and each induces DNA-to-protein cross-links (39–41). Although the biological significance of the lesions is not fully understood, several properties suggest that DNA-protein cross-links have the potential to cause mutations. These lesions are known to be relatively long-lived and, consequently, may be present during DNA replication (42); the lesion size may be a hindrance to enzymes that participate in DNA replication and repair, resulting in blockage on the DNA template. DNA processing has been shown to be blocked in *in vitro* systems by immobile proteins on DNA

(43, 44). The biological activity of photoactivated GV *in vitro*, such as in prophage induction and antitumor activity, is expressed at extremely low concentrations and UV doses (7) compared with those for other coumarin-based, UVB-activated compounds, such as the psoralens (30). This activity cannot be ascribed simply to DNA lesions, single-strand breakage, or intercalation (30). Also, unlike psoralens, this compound does not induce interstrand DNA cross-linking (16). It therefore appears that the most potent DNA damage induced by photoactivated GV is DNA-protein cross-linking. Given the specific interaction of photoactivated GV and GRP78, it is particularly interesting to note that a benzoquinone-based antitumor antibiotic, geldanamycin, specifically interacts with cytosol HSP-90. The antitumor activity of geldanamycin is due to the inhibition of tyrosine kinase activity, as seen in the Src family kinases. However, it does not directly bind Src kinase. It has been speculated that the mechanism is indirect and involves the interaction with HSP-90 that regulates the Src protein (45). Geldanamycin apparently binds to the pocket required to form the complex of HSP-90 and the target protein. The molecular action of photoactivated GV might also involve a protein that interacts with GRP78 and participates in signal transduction. It may be important to analyze the three-dimensional structure of GRP78 to search for a pocket for photoactivated GV. Otherwise, one could suppose that it is the covalent cross-linking of these principal target proteins *per se* that is responsible for GV activity and that the mechanism of action does not relate to the specific roles of these proteins in the cell.

## ACKNOWLEDGMENTS

We thank Dr. R. K. Elespuru for providing GV and Drs. T. Enomoto and Y. Fujiwara for encouragement.

## REFERENCES

1. Hatano, K., Higashide, E., Shibata, M., Kameda, Y., Horii, S., and Mizuno, K. Toromycin, a new antibiotic produced by *Streptomyces collinus*. Agric. Biol. Chem., *44:* 1157–1163, 1980.
2. Balitz, D., O'Herron, F., Bush, J., Vyas, D., Nettleton, D., Grulich, R., Bradner, W., and Doyle, T. Antitumor agents from *Streptomyces anandii*; gilvocarcins V, M and E. J. Antibiot. (Tokyo), *34:* 1544–1555, 1981.
3. Nakano, H., Matsuda, Y., Ito, K., Ohkubo, S., Morimoto, M., and Tomita, F. Gilvocarcins, new antitumor antibiotics. 1. Taxonomy, fermentation, isolation and biological activities. J. Antibiot. (Tokyo), *34:* 266–270, 1981.
4. Morimoto, M., Ohkubo, S., Tomita, F., and Marumo, H. Gilvocarcins, new antitumor antibiotic. 3. Antitumor activity. J. Antibiot. (Tokyo), *34:* 701–707, 1981.
5. Tomita, F., Takahashi, K., and Tamaoki, T. Gilvocarcins, new antitumor antibiotics. J. Antibiot. (Tokyo), *35:* 1038–1041, 1982.
6. Oyola, R., Arce, R., Alegria, A. E., and Garcia, C. Photophysical properties of gilocarcin V and M and their binding constant to calf thymus DNA. Photochem. Photobiol., *65:* 65–67, 1997.
7. Elespuru, R., and Gonda, S. Activation of antitumor agent gilvocarcins by visible light. Science (Washington DC), *223:* 69–71, 1984.
8. Greenstein, M., Monji, T., Yeung, R., Maiese, W. M., and White, R. J. Light-dependent activity for the antitumor antibiotic ravidomycin and desacetylravidomycin. Antimicrob. Agents Chemother., *29:* 861–866, 1986.
9. Peak, M. J., Peak, J. G., Blaumüller, C. M., and Elespuru, R. K. Photosensitized DNA breaks and DNA-to-protein crosslinks induced in human cells by antitumor agent gilvocarcin V. Chem. Biol. Interact., *67:* 267–274, 1988.
10. Bockstahler, L. E., Elespuru, R. K., Hitchins, V. M., Carney, P. G., Olvey, K. M., and Lytle, C. D. Inhibition of *Herpes* virus plaquing capacity in human diploid fibroblasts treated with gilvocarcin V plus near UV radiation. Photochem. Photobiol., *51:* 477–479, 1990.
11. Knobler, R. M., Radlwimmer, F. B., and Lane, M. J. Gilvocarcin V exhibits both equilibrium DNA binding and UV light induced DNA adduct formation which is sequence context dependent. Nucleic Acids Res., *20:* 4553–4557, 1992.
12. Gasparro, F., Knobler, R., and Edelson, R. The effects of gilvocarcin V and ultraviolet radiation on pBR322 DNA and lymphocytes. Chem. Biol. Interact., *67:* 255–265, 1988.
13. Tse-Ching, Y., and McGee, L. Light-induced modifications of DNA by gilvocarcin V and its aglycone. Biochem. Biophys. Res. Commun., *143:* 808–812, 1987.
14. McGee, L., and Misra, R. Gilvocarcin photobiology. Isolation and characterization of the DNA photoadduct. J. Am. Chem. Soc., *112:* 2386–2389, 1990.
15. Matsumoto, A., Vos, J-M., and Hanawalt, P. C. Repair analysis of mitocycin C-induced DNA crosslinking in ribosomal RNA genes in lymphoblastoid cells from Fanconi's anamia patients. Mutat. Res., *217:* 185–192, 1989.
16. Matsumoto, A., Fujiwara, Y., Elespuru, R. K., and Hanawalt, P. C. Photoactivated gilvocarcin D induces DNA-protein crosslinking in genes for human ribosomal RNA and dihydrofolate reductase. Photochem. Photobiol., *60:* 225–230, 1994.
17. Zhitkovich, A., and Costa, M. A simple sensitive assay to detect DNA-protein crosslinks in intact cells and *in vivo*. Carcinogenesis (Lond.), *13:* 1485–1489, 1992.
18. Costa, M., Zhitkovich, A., and Toniolo, P. DNA-protein cross-links in welders: molecular implications. Cancer Res., *53:* 460–463, 1993.
19. Laemmli, U. K. Cleavage of structural proteins during the assembly of the head of bacteriophage T4. Nature (Lond.), *227:* 680–685, 1970.
20. Schägger, H., and von Jagow, G. Tricine-sodium dodecyl sulfate-polyacrylamide gel electrophoresos for the separation of proteins in the range from 1 to 100 kDa. Anal. Biochem., *166:* 368–379, 1987.
21. LeGendre, N., and Matsudaira, P. Purification of proteins and peptides by SDS-PAGE. *In:* P. Matsudaira (ed.), A Practical Guide to Protein and Peptide Purification for Microsequencing, pp. 49–69. San Diego, CA: Academic Press, 1989.
22. Brodsky, J. L., and Schekman, R. Heat shock cognate proteins and polypeptide translocation across the endoplasmic reticulum membrane. *In:* L. Nover (ed.), Heat Shock Response of Eukaryotic Cells, pp. 85–109. Berlin: Springer-Verlag, 1984.
23. Haas, I. G., and Wabl, M. Immunogloblin heavy chain binding protein. Nature (Lond.), *306:* 387–389, 1983.
24. Shiu, R. P., Pouyssegur, J., and Pastan, I. Glucose depletion accounts for the induction of two transformation-sensitive membrane proteins in Rous sarcoma virus-transformed chick embryo. Proc. Natl. Acad. Sci. USA, *74:* 3840–3844, 1977.
25. Kozutsumi, Y., Normington, K., Press, E., Slaughter, C., Sambrook, J., and Gething, M-J. Identification of immunoglobulin heavy chain binding protein as glucose-regulated protein 78 on the basis of amino acid sequence, immunological cross-reactivity, and functional activity. J. Cell Sci. (Suppl.), *11:* 115–137, 1989.
26. Nishikawa, S., Hirata, S., and Nakano, A. Inhibition of endoplasmic reticulum (ER)-to-Golgi transport induces relocalization of binding protein (BiP) within the ER to form the BiP bodies. Mol. Biol. Cell, *5:* 1129–1143, 1994.
27. Bhattacharyya, T., Karnezis, A. N., Murphy, S. P., Hoang, T., Freeman, B. C., Phillips, B., and Morimoto, R. I. Cloning and subcellular localization of human mitochondrial hsp 70. J. Biol. Chem., *270:* 1705–1710, 1995.
28. Munro, S., and Pelham, H. R. An hsp70-like protein in the ER: identity with the 78 kd glucose-regulated protein and immunoglobulin heavy chain binding protein. Cell, *46:* 291–300, 1986.
29. Pelham, H. R. Hsp 70 accelerates the recovery of nuclear morphology after heat shock. EMBO J., *3:* 3095–3100, 1982.
30. Elespuru, R. K., and Look, S. A. Gilvocarcin V, a photodynamic DNA damaging agent of unusual potency. *In:* D. C. Neckers (ed.), New Directions in Photodynamic Therapy, pp. 107–114. Bellingham, United Kingdom: The International Society for Optical Engineering, 1987.
31. Wolffe, A. P. New insights into chromatin factors in transcriptional control. FASEB J., *6:* 3354–3361, 1992.
32. Felsenfeld, G. Chromatin as an essential part of the transcriptional mechanisms. Nature (Lond.), *355:* 219–224, 1992.
33. Zweidler, A. Core histone variants of the mouse: primary structure and different expression. *In:* G. S. Stein, J. L. Stein, and W. F. Marzluff (eds.), Histone Genes, pp. 339–369. New York: John Wiley & Sons, Inc., 1994.
34. Wolffe, A. P. Transcription. In tune with the histones. Cell, *77:* 13–16, 1994.
35. Mann, R. K., and Grunstein, M. Histone H3 N-terminal mutations allow hyperactivation of the yeast *GAL1* gene *in vivo*. EMBO J., *11:* 3297–3306, 1991.
36. Mahadevan, L. C., Willis, A. C., and Barratt, M. J. Rapid histone H3 phosphorylation in response to growth factors, phorbol esters, okadaic acid, and protein synthesis inhibitors. Cell, *65:* 775–783, 1991.
37. Singer, B., and Grunberger, D. Reactions of directly acting agents with nucleic acids. *In:* B. Singer and D. Grunberger (eds.), Molecular Biology of Mutagens and Carcinogens, pp. 53–55. New York: Plenum Publishing Corp., 1983.
38. Miller, C. A., III, and Costa, M. Analysis of proteins crosslinked to DNA after treatment of cells with formaldehyde, chromate and *cis*-diaminedichloroplatinum (II). Mol. Toxicol., *2:* 11–26, 1989.
39. Sellakumar, A. R., Snyder, C. A., Solomon, J. J., and Albert, R. E. Carcinogenicity of formaldehyde and hydrogen chloride in rats. Toxicol. Appl. Pharmacol., *81:* 401–406, 1985.
40. Hertel, R. F. Sources of exposure and biological effects of chronium. *In:* I. K. O'Neill, P. Schuller, and L. Fishbein (eds.), IARC Monogram Environmental Carcinogens-Selected Methods of Analysis, pp. 63–77. Oxford, United Kingdom: Oxford University Press, 1986.
41. Kempf, S. R., and Ivanovic, S. Chemotherapy-induced malignancies in rats after treatment with cisplatin as a single agent and in combination: preliminary results. Oncology (Basel), *43:* 187–191, 1986.
42. Sigiyama, M., Patierno, S. R., Cantoni, O., and Costa, M. Characterization of DNA lesions induced by $CaCrO_4$ in synchronous and acynchronous cultured mammalian cells. Mol. Pharmacol., *29:* 606–613, 1986.
43. Bedinger, P., Hochstrasser, M., Jongneel, C. V., and Alberts, B. Properties of the T4 bacteriophage replication apparatus: the T4 dda DNA helicase is required to pass a bound RNA polymerase molecule. Cell, *34:* 115–123, 1983.
44. Donahue, B. A., Yin, S., Taylor, J-S., Reines, D., and Hanawalt, P. C. Triplet change by RNA polymerase II arrested by a cyclobutane pyrimidine dimer in the DNA template. Proc. Natl. Acad. Sci. USA, *91:* 8502–8506, 1994.
45. Whitesell, L., Mimnaugh, E. G., De Costa, B., Myers, C. E., and Neckers, L. M. Inhibition of heat shock protein HSP90-pp60$^{v\text{-}src}$ heteroprotein complex formation by benzoquinone ansamycins: essential role for stress proteins in oncogenic transformation. Proc. Natl. Acad. Sci. USA, *91:* 8324–8328, 1994.

# Histone H3 and Heat Shock Protein GRP78 Are Selectively Cross-Linked to DNA by Photoactivated Gilvocarcin V in Human Fibroblasts

Akira Matsumoto and Philip C. Hanawalt

*Cancer Res* 2000;60:3921-3926.